

Late Holocene Earthquakes on the Aeropuerto Fault, Managua, Nicaragua

by Hugh Cowan,* Carol Prentice, Daniela Pantosti, Paolo de Martini, Wilfried Strauch,
and Workshop Participants

Abstract Managua, capital of Nicaragua, is built on the shore of Lake Managua, within a densely faulted graben at a major discontinuity in the Central American volcanic chain. Shallow moderate earthquakes (M_s 6–6.2) ruptured faults with devastating effect at the heart of urban Managua in 1931 and 1972, and damaging earthquakes are cataloged in the earlier history of the surrounding region. The Aeropuerto fault is a major structure in the Managua Graben, but like other faults in this area its behavior is little understood. Paleoseismic investigations now suggest that the most recent large earthquake on this fault occurred sometime during the interval A.D. 1650–1810. An earlier earthquake on this fault occurred prior to A.D. 1390 and possibly around 2000 B.P.

On the basis of stratigraphic correlations we estimate the ages of two shorelines associated with former high stands of Lake Managua to be less than 6.4 ka and approximately 2 ka, respectively. Deformation of these abandoned shorelines adjacent to the Aeropuerto fault implies a vertical slip rate of 0.3 to 0.9 mm/yr. Strike-slip movement on this fault is also expected, but no direct measurement could be performed. By comparison with faults of similar geometry in the Managua area that ruptured in 1931 and 1972, we suspect a left-lateral component of horizontal slip that is higher than the vertical one but less than 5 mm/yr.

Additional data on slip rate and timing of paleoearthquakes are needed to better assess the Holocene behavior of the Managua faults and to investigate the influence of magmatic processes on the nature of faulting in the Managua Graben.

Introduction

Managua, capital of Nicaragua, is built on the shore of Lake Managua, within a densely faulted graben and located at a major discontinuity in the Central American volcanic chain (Fig. 1). The volcanic chain is a NW–SE trending alignment of stratocone and shield volcanoes associated with the Cocos–Caribbean plate boundary at the Pacific margin of Nicaragua. The Cocos plate is convergent with the Caribbean plate at a rate of about 8 cm/yr (DeMets *et al.*, 1994) and is subducted steeply to about 200 km beneath the volcanic chain (Hernandez *et al.*, 1994; Protti *et al.*, 1995). The volcanic chain is situated on a back-arc lowland (Nicaragua Depression) that extends from El Salvador to Costa Rica and separates Tertiary igneous rocks of the interior highlands from marine sedimentary rocks of the Pacific coastal hills (Instituto Geográfico Nacional, 1972; Mann *et al.*, 1990). Two large lakes (Lake Managua and Lake Nicaragua) and a substantial volume of Quaternary volcanoclastic material occupy the Nicaragua Depression, but only a short (70 km) section of the Nicaragua Depression west of Managua is bounded by a prominent fault (Mateare fault; Fig. 1).

In the Managua area, where there is abundant evidence of recent faulting, a graben (Managua Graben) has formed at a 15-km discontinuity in the strike of the volcanic chain, from Apoyeque Caldera to Masaya Caldera, southeast of the metropolitan area (Fig. 1). The Managua Graben and its strike-slip and oblique-normal faults show evidence of mild east–west extension and left-lateral strike slip along a north and northeast trend (Figs. 1, 2). The NNE–SSW trending Tiscapa fault and three adjacent, parallel faults, all exhibited left-lateral and minor normal displacement during the 23 December 1972, M 6.2 earthquake. Aggregate horizontal movements were in the range of 2 to 38 cm, down to the ESE (Brown *et al.*, 1973; Ward *et al.*, 1974). In 1931 an M 6.0 earthquake ruptured the Estadio fault, 1.5 km west of the Tiscapa fault, with a maximum observed normal slip of 10 cm and an undefined component of strike slip (Sultan, 1931; White and Harlow, 1993).¹

*Present address: Institute of Geological and Nuclear Sciences, P.O. Box 30-368, Lower Hutt, New Zealand, (h.cowan@gns.cri.nz.)

¹The 31 March 1931 and 23 December 1972 earthquakes in Managua resulted in approximately 2500 and 11,000 deaths, respectively. More than 200,000 persons were left homeless in 1972, and economic losses exceeded 40% of gross national product in that year (Coburn and Spence, 1992).

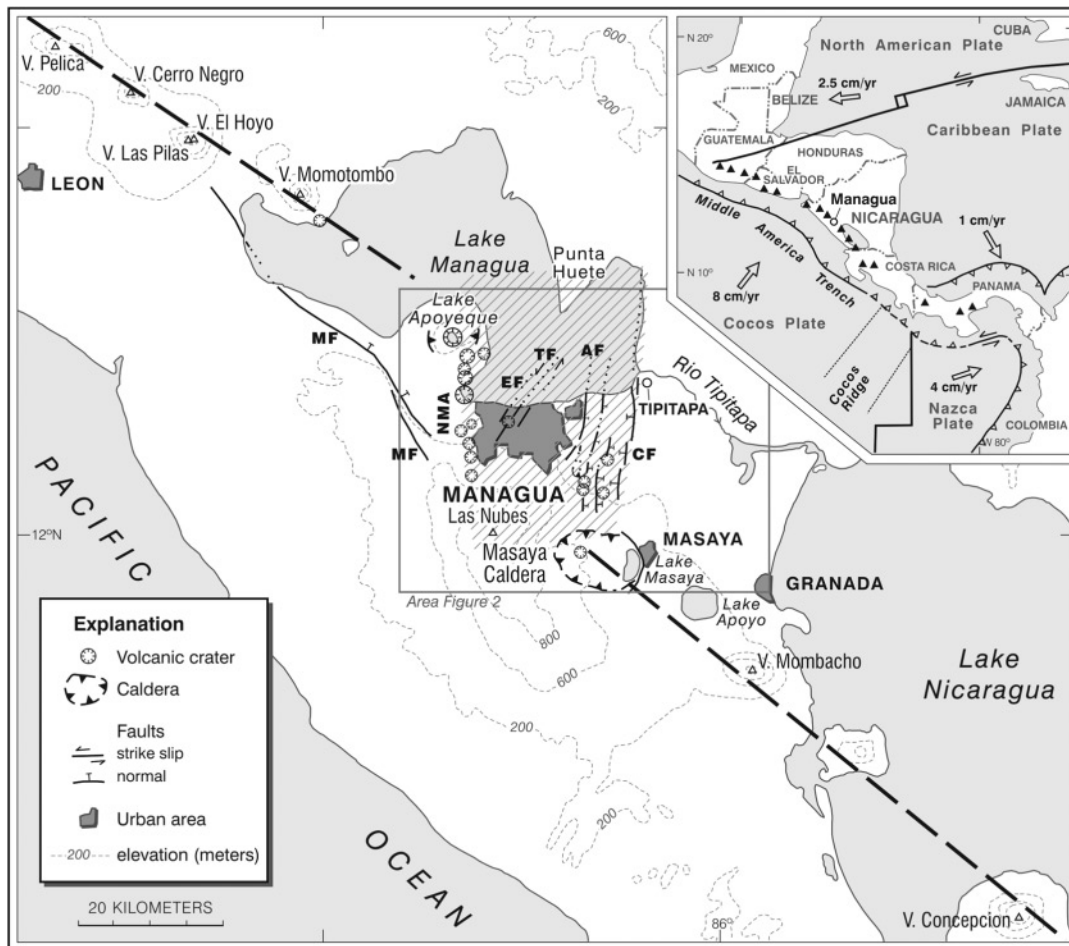


Figure 1. Map of region around Managua, Nicaragua, showing the discontinuity in the strike of the volcanic chain (heavy dashed line) associated with the Managua Graben, whose approximate limits are indicated by the diagonal hatch. Major structural elements include: MF, Mateare fault; EF, Estadio fault; TF, Tiscapa fault; AF, Aeropuerto fault; CF, Cofradia fault; NMA, Nejapa–Miraflores–Apoyeque alignment. Inset shows plate tectonic setting.

The western margin of the Managua Graben is defined by cinder cones and collapse pits that extend south from the Apoyeque Caldera along a trend known as the Nejapa–Miraflores–Apoyeque alignment (e.g., Bice, 1980) (Fig. 2). The Asoscosca–Acahualinca and San Judas fault zones form east-facing escarpments at this margin of the graben, and Holocene displacements are documented at several localities (Woodward-Clyde Associates, 1975) (Table 1). The eastern margin of the Managua Graben and Lake Managua are defined by the Cofradia fault. The Cofradia fault forms a prominent escarpment that extends south in right-stepping en echelon sections to the Masaya Caldera (Fig. 2), a large shield volcano and source of voluminous Holocene eruptions and frequent historical activity (Bice, 1980; Williams, 1983). The floor of the Managua Graben is at its lowest elevation west of the Cofradia fault and is marked by small volcanic cones, craters, and multiple unnamed faults along its axis farther south. We informally refer to this deepest part

of the Managua Graben as the Airport graben. The Aeropuerto fault forms a prominent, 20-km-long scarp south of Lake Managua and defines the western boundary of the Airport graben (Fig. 2).

The floor of the Managua Graben rises gently southward from the shore of Lake Managua and is underlain by volcanoclastic deposits of Holocene (<10 ka) to late Pleistocene (10–30 ka) age. The deposits have been traced to the cinder cones and collapse pits along the Nejapa–Miraflores–Apoyeque alignment to the west (Bice, 1980), and the Masaya Caldera to the southeast (Williams, 1983). Farther south, the topography rises steeply to more than 900 m across the Mateare fault and is underlain by voluminous ignimbrite sheets and mudflows erupted from a former caldera structure in the Masaya area prior to about 30,000 years ago (Sussman, 1985). These deposits form the local basement geology, and some of the flows extend northward up to 50 km from the source (van Wyk de Vries, 1993).

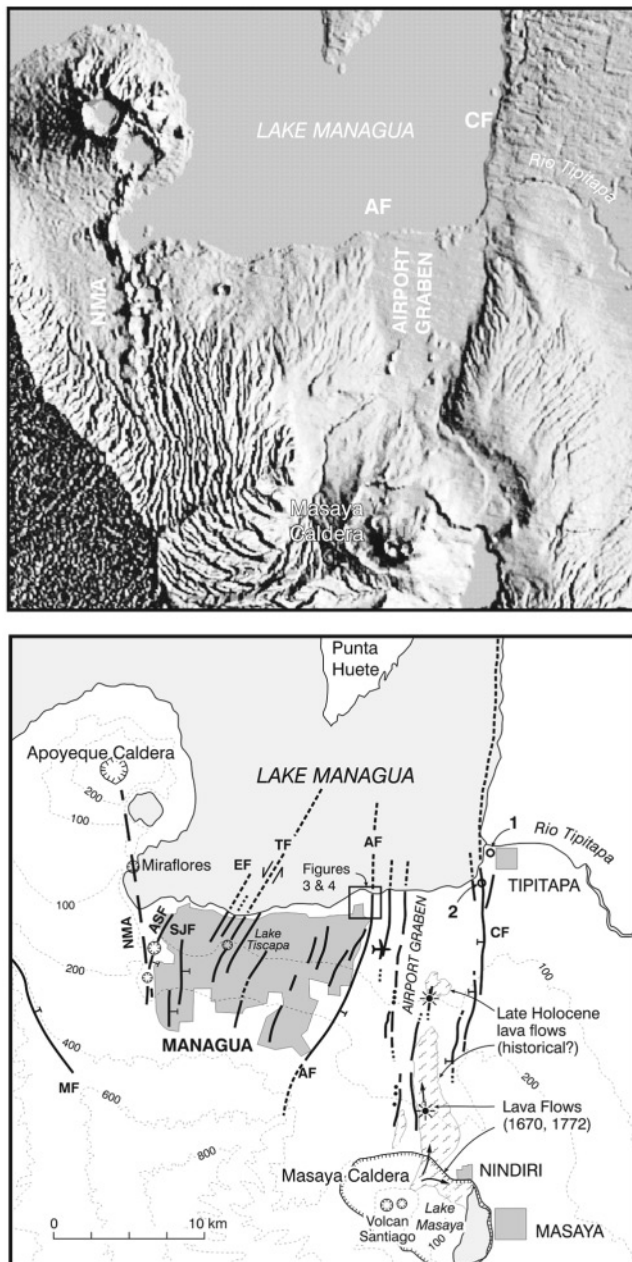


Figure 2. (top) Digital elevation model (DEM) of Managua area showing the deepest part of the Managua Graben lies between the Aeropuerto (AF) and Cofradia (CF) faults. We informally call this the Airport graben. (bottom) Interpretive map based on the DEM, our field mapping, and earlier studies (Woodward-Clyde Associates, 1975; Dames and Moore-Lamsa, 1978; Cowan *et al.*, 2000) showing major faults and volcanic features. ASF, Asososca–Acahualinca fault zone; SJF, San Judas fault zone. Other abbreviations as in Fig. 1.

Fault Kinematics

Faults transverse to the volcanic chain are more prominent at Managua than elsewhere along the arc, and possible kinematic relationships to the driving plate-boundary forces have been debated for several decades (review in Mann *et al.*, 1990). Possibilities include right-lateral, strike-slip faulting parallel to the volcanic chain (e.g., McBirney and Williams, 1965; Carr, 1976; White, 1991; Weinberg, 1992), or transverse breaks in the subducted Cocos plate accounting for the lateral discontinuity in the strike of the volcanic chain across Managua (e.g., Stoiber and Carr, 1973). Another alternative is that Managua Graben faults represent oceanic-type transform faults connecting the ends of two offset and widening volcanic centers (e.g., Dewey and Algermissen, 1974). Alternative models proposed by Malfait and Dinkelman (1972) and Manton (1987) involve block rotations and eastward motion of the Caribbean plate in response to movements along the Caribbean–North America plate boundary.

Studies of seismicity have concluded that there is no evidence for sharp breaks in the subducted Cocos plate (Bevis and Isacks, 1984; Hernandez *et al.*, 1994; Protti *et al.*, 1995), but there are few data available to resolve the kinematics of shallow faulting. Available geological information from faults at the northern margin of the Nicaragua Depression reportedly indicate no evidence of recent movement (van Wyk de Vries, 1993). Shallow earthquakes recorded during a period of fairly robust local network coverage (1975–1982) indicate that most microseismicity during this period was associated with the Tiscapa fault aftershock activity with little, if any activity, located near the Mateare, Cofradia, or Aeropuerto faults (Hernandez *et al.*, 1994). However, the Cofradia and Aeropuerto faults have clear topographic expression in Holocene deposits. Their length and proximity to other historically active faults suggest that they may contribute significantly to the seismic hazard in the Managua area. Previous investigations of the Cofradia fault have revealed evidence of surface displacement in the last few thousand years near Tipitapa (Dames and Moore-Lamsa, 1978).

Aeropuerto Fault

The purpose of our study is to determine the timing and nature of Late Holocene faulting associated with the Aeropuerto fault and to estimate a preliminary slip rate for this source. Although this fault was first identified several decades ago based on its surface expression across young landforms (Woodward-Clyde Associates, 1975), little is known about the nature of the Aeropuerto fault, its role in the regional tectonics of the Managua Graben, or its contribution to seismic hazard.

Within and west of the Airport graben are two former shorelines of Lake Managua, situated 3 to 4 m above the modern lake level (shorelines 1 and 2, Fig. 3). No higher shorelines have been reported in this region. Shoreline 1

Table 1
Summary Descriptions of Principal Faults, Managua, Nicaragua

Code	Fault Zone	Strike and Projected Length	Maximum Individual Reported	Displacement			Age of Most Recent Movement (kyr = 10 ³ yr)	Comments	References*
				Maximum Scarp Height	Observed Sense of Movement	Slip Rate (mm/yr)			
MF	Mateare	N50°W, ±318° 35 km to max. 70 km	Unknown	~200 m	Large component down to northeast	Unknown	Probably <20 kyr	NE-facing topographic escarpment in late Pleistocene ignimbrite deposits. No Holocene faulting reported and seismically quiescent since 1975 or longer.	1, 4, 8
NMA	Nejapa–Miraflores–Apoyeque Alignment	N10°W, ±5° ~20 km	~1 m normal	~80 m	Down to east	Unknown	Probably <10 kyr	Arcuate scarps associated with volcanic craters defining the western margin of the Managua Graben.	2, 3, 8
ASF	Asososca–Acahualinca	N30°E, ±10° 5 km	~3 m normal	20 m	Mainly down to east, few scarps down to west	Unknown	<10 kyr	Arcuate east- and west-facing scarps that intersect the NMA to the south.	2, 3, 8
SJF	San Judas	N–S, ±5° 5 km to max. 10 km	1 m normal	15 m	Down to east	Unknown	Probably <5 kyr	Arcuate east-facing scarp that displaces Holocene soil. Minor cracking during 1972 earthquake.	2, 3, 8
EF	Estadio	N30°E, ±5° 2 km on land to max. 10 km beneath Lake Managua	0.5 m normal	~1 m normal	Left-lateral strike-slip and down to east	Unknown	31 March 1931	Surface rupture along a 2-km section of the fault in 1931. Minor cracking during 1972 earthquake.	1, 5, 8
TF	Tiscapa	N24°E, ±7° 10 km to max. 20 km beneath Lake Managua	3.5 m normal	20 m normal	Left-lateral strike-slip and down to east	Probably 0–5	23 December 1972	Little geomorphic expression in former downtown area, but left-lateral offset of several meters on northeast wall of Laguna de Tiscapa. Farther SW an east-facing scarp up to 20 m high.	1, 2, 8
AF	Aeropuerto	N3°E, ±6° ~15 km plus extension beneath Lake Managua	0.5–1 m normal	10–12 m normal	Down to east Strike-slip may be important	Probably 0–5	A.D. 1650–1810	Surface trace slightly convex to the east and the fault subvertical. Scarp has maximum height of 10–12 m west of the Airport.	6, 8
CF	Cofradia	N4°E, ±13° ~40 km	0.5–1 m normal	~15 m	Down to west	Probably 0–5	<5 kyr based on offset lake deposits near Tipitapa	Prominent escarpment extends south to the Masaya caldera and is associated with numerous hot springs.	7, 8

*1, Brown *et al.* (1973); 2, Woodward-Clyde (1975); 3, Bice (1980); 4, Hernandez *et al.* (1994); 5, Sultan (1931); 6, this study; 7, Dames and Moore-Lamsa (1978); 8, Cowan *et al.* (2000).



Figure 3. Map of field area showing shorelines 1 and 2, based on analysis of aerial photographs (Geographic Air Survey Ltd. 1996) and field mapping. T1, T2, and T3 indicate locations of trenches excavated across the Aeropuerto fault. Topographic profiles crossing the fault scarp are labeled p1, p2, p3, and p4. Star symbol indicates location of streambank exposure shown in Fig. 8. Spot elevations from INETER (1987).

forms a prominent erosional cliff about 3 m high, which extends for several kilometers along the edge of metropolitan Managua and is present only west of the Aeropuerto fault (Fig. 3; cf. Fig. 4). The younger shoreline 2 is marked by a low, narrow berm, about 1 to 2 m high, composed of reworked volcanic sand. This ridge separates the north-sloping surface of the most recently abandoned lakebed from an older lakebed to the south.

We analyzed aerial photographs taken in 1986 and 1996, conducted field mapping and topographic profiling, and excavated three trenches at two sites near the northern end of the Aeropuerto fault, close to its intersection with Lake Managua. We also studied and logged a natural stream-

bank exposure that occurs between the two shorelines. We chose this region because the two former lake shorelines indicated the presence of young lakebeds that have been disrupted by the fault. We mapped these shorelines and constructed a leveling profile (p1 in Figs. 3 and 9) along the younger one (shoreline 2) to provide information regarding its deformation across and adjacent to the fault. We have proposed a correlation among the deposits exposed in the three trenches and the streambank exposure, and this correlation is reflected in the unit numbering system we have adopted. For example, unit S-7, exposed in the streambank exposure is suggested to correlate to unit T1-7, exposed in trench 1.



Figure 4. Stereo air-photo pair of field area illustrated in Fig. 3, showing shorelines 1 and 2 and the Aeropuerto fault. (Photo Run N4, scene 86-3 and 86-4, INETER photo library).

Excavations across the Aeropuerto Fault

Trench 1

Site T1 is located along a low scarp produced by the Aeropuerto fault. On the downthrown side of the scarp is a small stream and marshy area, where sediments are being deposited and organic materials are accumulating. The trench excavated at site T1 (Fig. 3) exposed a section of volcanic units overlain by peat and organic-rich silt layers (Fig. 5). These units are displaced across a zone of closely spaced, vertical to subvertical faults that do not appear to extend all the way to the ground surface; however, the fault scarp is distinct on the ground surface, so the fact that the faults do not appear to extend to the surface is most likely due to bioturbation of the near-surface deposits. The youngest faulted horizon (unit T1-3A) contains pottery fragments, charcoal, and peat. Radiocarbon analysis of three samples (1, 2, and 3 in Table 2) shows that the upper part of the section is less than 740 years old.

Beneath these youngest sediments is reworked volcanic agglomerate (unit T1-7A), which contains abundant plant fossils and is capped by a strongly calcified siltstone (calcrete, unit T1-4) and soil on the west side of the Aeropuerto fault. The agglomerate is correlated across the fault and displays about 2 m of vertical separation across the fault zone. We could not establish any definite component of strike-slip offset; however, the subvertical dips are indicative of a strike-slip fault, consistent with dips of the Aeropuerto fault exposed in a quarry west of the international airport (Fig. 2, bottom) and those of the Tiscapa and Estadio faults farther

west (Woodward-Clyde Associates, 1975). Also suggestive of strike-slip faulting are the thickness changes of units T1-7A and T1-7B across the fault, although because these units are not exposed right at the fault zone on the downthrown side, this observation does not provide definitive evidence of strike-slip displacement.

There is evidence for at least two fault rupture events in trench 1. The most recent earthquake faulted the entire sedimentary sequence up through the unit T1-4–unit T1-3 contact across faults F3, F4, and F5, and displacing the deposits that contain radiocarbon samples 1, 2, and 3. Samples 2 and 3 were collected from units deposited by fluvial overbank processes, and were not redeposited after the event in a fissure or colluvial deposit. The depositional setting of sample 1 is less clear, and this sample could be part of a colluvial unit. We interpret the numerous faults and fractures that break through unit T1-7 and terminate below unit T1-4 to represent at least one earlier earthquake that occurred prior to the formation of unit T1-4. The difference in depositional environment on either side of the fault zone, reflected by the formation of unit T1-4 southwest of the fault and the deposition of unit T1-5 northeast of the fault, provides further evidence for an event at this time. Unit T1-4 formed on the uplifted block and blanketed the scarp, and fluvial overbank deposition with no soil formation (unit T1-5) occurred on the downthrown side.

Trenches 2 and 3

Trenches 2 and 3 are located about 300 m north of trench 1 and are directly north of shoreline 2 (Fig. 3). No

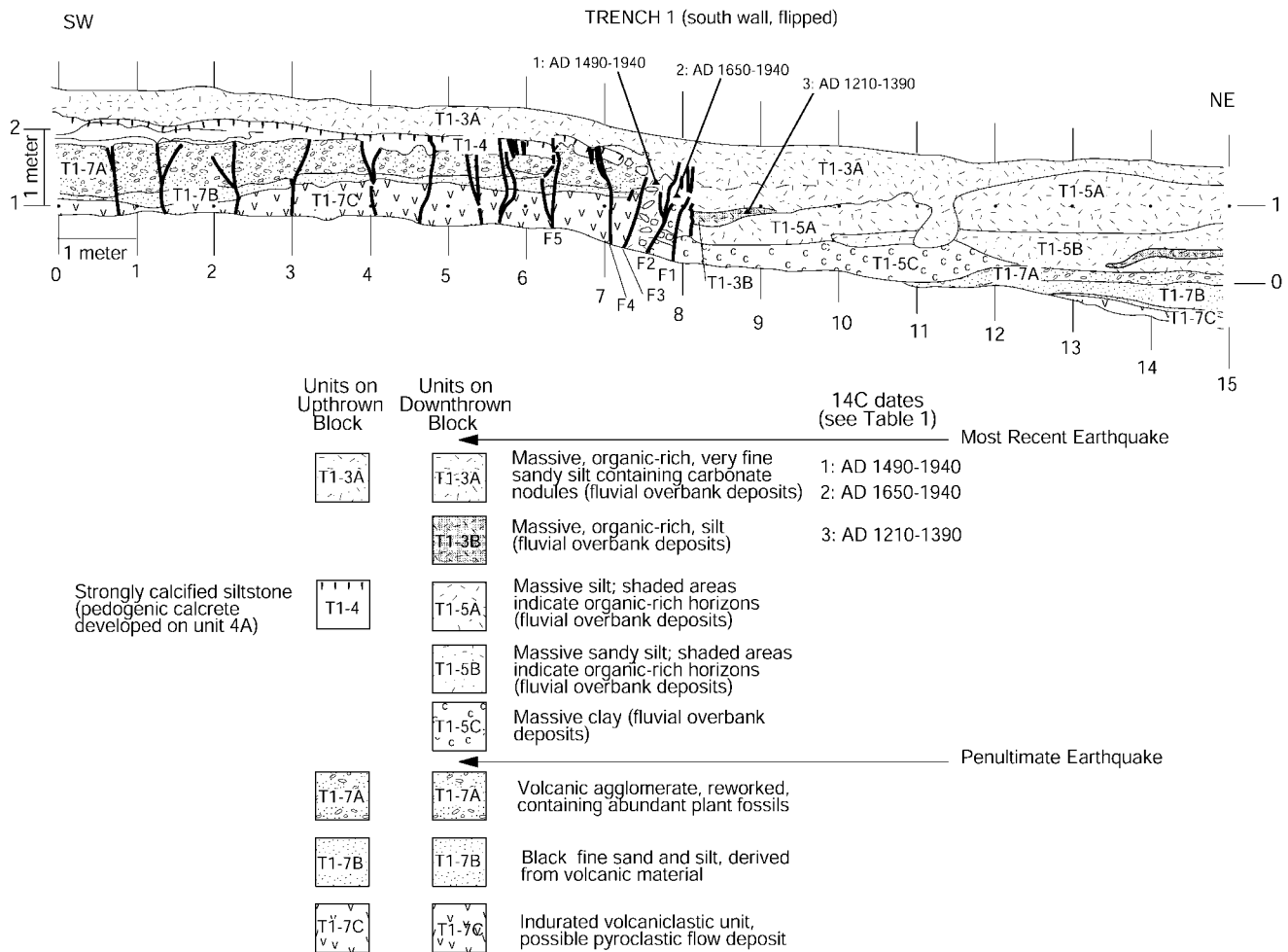


Figure 5. Log of trench 1, showing evidence for two surface-rupturing earthquakes. The most recent event occurred after the deposition of the unit containing sample 2, which formed after 1650 A.D. Although this trench does not provide a minimum limiting date for this event, samples collected from trenches 2 and 3 (see Figs. 5 and 6) indicate that the most recent surface rupture occurred prior to A.D. 1810. Units exposed in this trench include faulted volcaniclastic units (T1-7A, T1-7B, and T1-7C) and overlying fluvial and overbank units composed of sand, silt, and clay (units T1-3 and T1-5). Shaded units represent organic-rich horizons. Unit T1-4 is a strongly calcified siltstone (calcrete). The most recent surface-rupturing event displaced unit T1-4 across faults labeled F3, F4, and F5. Faults labeled F1 and F2 also broke during this event, displacing units containing radiocarbon samples 1, 2, and 3. Most of the faults southwest of F5 do not displace unit T1-4. We interpret these as evidence of an earlier event that occurred prior to the formation of units T1-4 and T1-5 and after the deposition of unit T1-7A.

scarp is present at this location along the projected trend of the fault scarp mapped south of shoreline 2; however, 3 to 4 m west of the location of the fault is a sinuous scarp about 0.5 m high, formed in strongly lithified volcanic agglomerate that forms the youngest abandoned lakebed associated with shoreline 2 (Fig. 3). This scarp is the result of vertical displacement of the former lakebed across the Aeropuerto fault, but its location and trend diverge from that of the fault, indicating a westward retreat of the scarp due to fluvial or lake shore erosion (or both). These relations indicate that the fault is buried at this location, and we expected that unfaulted fluvial sediments would cap the most recent fault rupture,

providing an opportunity to determine a minimum age for the most recent surface rupture.

We excavated two trenches (T2 and T3) across the fault, to provide more exposures to work with at this site (Fig. 3). The two trenches were only a few meters apart and exposed similar stratigraphic sections comprising unfaulted fluvial layers overlying a faulted sequence of reworked volcanic agglomerate and finely laminated lake sediments (Figs. 5 and 6). The uppermost fluvial layer (unit T2/3-1) contains contemporary artifacts (plastic and glass), whereas the lower fluvial layer (unit T2/3-2) contains abundant pottery shards and fragments of baked roof tiles. Three charcoal samples

Table 2
Calculated Dates From ^{14}C Analysis of Charcoal and Peat, Aeropuerto Fault, Managua, Nicaragua

No.	Sample	Delta ^{13}C (0/00)	^{14}C age* (yr B.P.)	Calendar date [†] (A.D. if unlabeled)	Calibrated years B.P.	Probability distribution (A.D.)	Stratigraphic significance	Material
1	T1S1 AA-32704	-26.0	260 ± 40	1490–1950	10–460	1490–1610.39 1610–1680.45 1760–1800.15 1930–1940.01		charcoal
2	T1S2 Beta-117480	-25.6	170 ± 50	1650–1940	10–300	1650–1890.85 1910–1940.15	predates most recent event	peat
3	T1S3 AA-32705	-27.1	720 ± 55	1210–1390	560–740	1210–1340.79 1350–1390.21	postdates penultimate event	charcoal
4	T2N2 AA-32706	-26.7	245 ± 45	1490–1940	10–430	1490–1600.24 1610–1810.70 1920–1940.05	postdates most recent event	wood
5	T2N3a AA-32707	-29.1	205 ± 45	1630–1950	0–420	1530–1540.01 1630–1710.28 1720–1880.58 1910–1950.13	postdates most recent event	woody peat
6	T3N20 Beta-117481	-29.0	170 ± 40	1660–1950	0–290	1660–1710.19 1720–1880.64 1910–1950.17	postdates last surface rupture	charcoal
7	Section/unit IV Beta-117479	-26.8	1970 ± 40	50 B.C.–A.D. 120	1830–1990		approximate age of shoreline 2	charcoal
8	T3W1 Beta-117482	-28.5	5550 ± 50	4490 B.C.–4260 B.C.	6440–6210		approximate age of shoreline 1	organic silt

*Conventional radiocarbon ages reported by Beta Analytic (samples labeled Beta-xx) or University of Arizona (samples labeled AA-xx). Calculations assume a Libby half-life (5568 yr). Uncertainties are 1 standard deviation counting errors.

[†]Dendrochronologically calibrated, calendar age ranges from CALIB Rev. 4.2, Method B, 2 standard deviation uncertainty. Rounded to nearest decade. Stuiver *et al.* (1998).

(4, 5, and 6; Table 2) collected from unit T2/3-2 provide radiocarbon ages indicating that these sediments were deposited within the last several hundred years. Beneath the erosional contact at the base of unit T2/3-2, coarse, strongly lithified, reworked volcanic agglomerate (unit T2/3-6) of the former lakebed overlies finely laminated lake sediments (unit T2/3-8). The lake sediments contain freshwater mollusks and extend westward beneath the former shoreface of shoreline 2 (Fig. 5 and 6). Both the agglomerate and the lake sediments are faulted and display normal separation down to the east.

Discussion

Timing of the Most Recent Earthquake on the Aeropuerto Fault

Results from the three excavations provide evidence for the most recent surface rupture and constraints on its age. Based on sample 2 from trench 1, this event occurred sometime after 1650 A.D. (Fig. 5; Table 2). Samples 4 and 6 from trenches 2 and 3 postdate the most recent earthquake and

thus provide minimum ages for this event (assuming the sample ages are approximately the same as the age of the sediment in which they are deposited). The full 2-sigma calibrated age ranges for both of these samples extend to the present (A.D. 1490–1940 and 1660–1950, respectively). The probability distribution for sample 4 indicates that the A.D. 1920–1940 age range is unlikely, having a probability of only 5%. In addition, because relations in trench 1 show that this event occurred after A.D. 1650, we can also rule out the earliest interval for sample 4 (A.D. 1490–1600). Thus, the interval A.D. 1610–1810 is the probable interval for the age of sample 4, indicating that the most recent earthquake occurred before A.D. 1810. This is consistent with the probability distributions for samples 5 and 6 (Table 2).

An interval A.D. 1650–1810 for the most recent surface rupture on the Aeropuerto fault indicates that this was a historical event. There are a number of earthquakes reported from Nicaragua during that time interval, but the largest earthquakes reported in the Managua region are those of 1663, 1764, and 1772 (Leeds, 1974), coinciding with volcanic unrest and eruptions from Masaya Caldera.

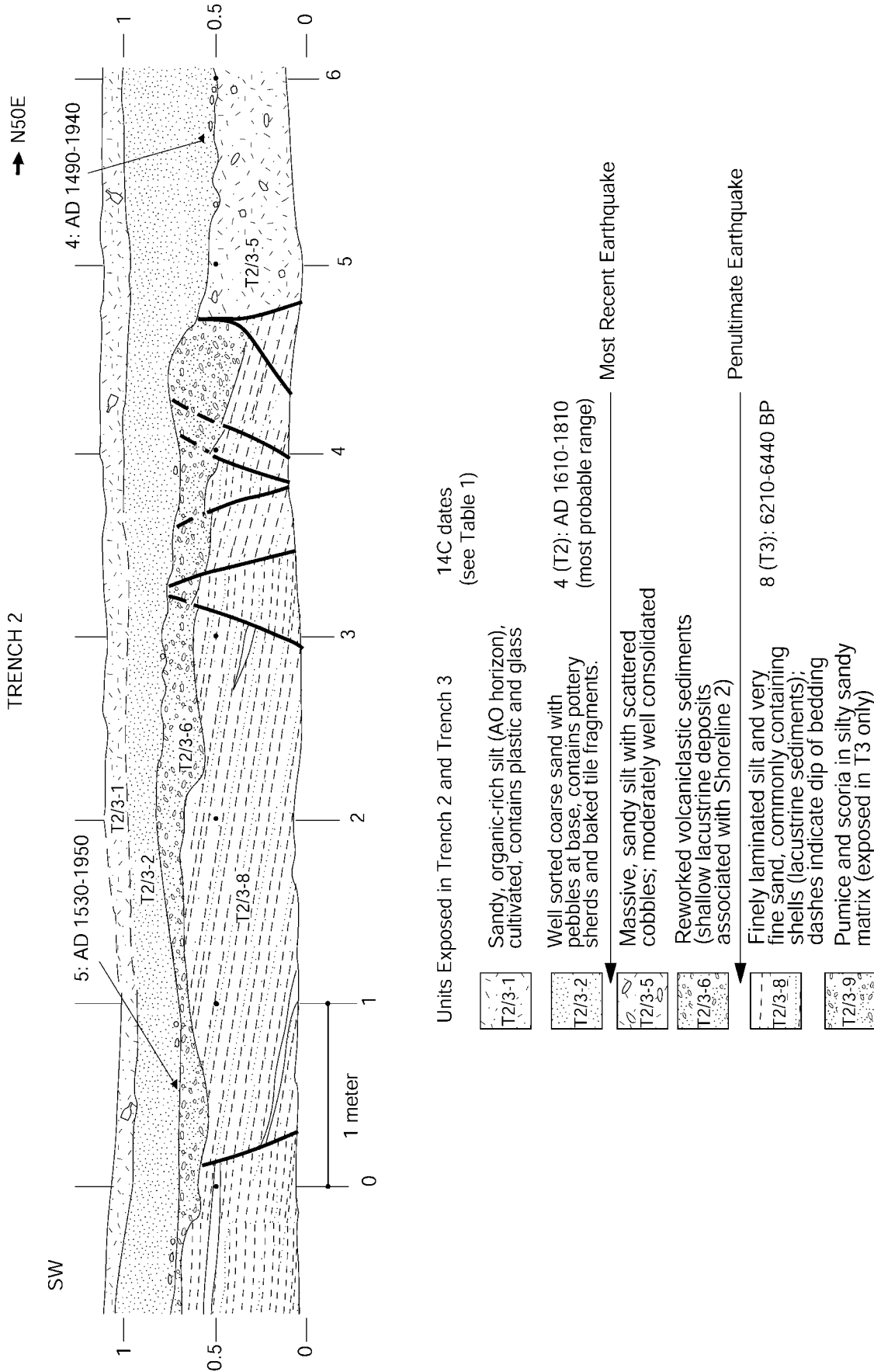


Figure 6. Log of trench 2 (for trench 3, see Fig. 7), showing strong evidence for the most recent surface-rupturing earthquake, and some evidence suggesting an earlier event. The most recent event is represented by numerous faults that displace unit T2/3-6 but do not displace unit T2/3-2. The ages of radiocarbon samples 4, 5, and 6 all indicate that unit T2/3-2 was deposited within the last few hundred years. Analysis and comparison of the probability distributions for the radiocarbon analyses from all three trenches indicate that the most recent surface-rupturing earthquake probably occurred between A.D. 1650 and 1810. Units exposed in these trenches include lacustrine beds (unit T2/3-8) containing a radiocarbon sample that dates to 6210–6400 calibrated years B.P. The lacustrine beds are overlain by reworked volcaniclastic deposits (unit T2/3-6) and unfaulted fluvial deposits (units T2/3-1 and T2/3-2). The fault between meters 0 and 1 in trench 2 and meters 3 and 4 in trench 3 breaks unit T2/3-8, but not unit T2/3-6, suggesting that an earlier event may have occurred prior to the deposition of unit T2/3-6. This earlier event is most likely the same event we interpret from relations in trench 1.

Timing of the Penultimate Earthquake on the Aeropuerto Fault

The age of the penultimate earthquake is poorly constrained in trench 1 by the radiocarbon date of sample 3 (Fig. 5; Table 2). This sample postdates the penultimate earthquake, because it was collected from unit T1-3B, which overlies unit T1-7A, and the penultimate event horizon is at the top of unit T1-7A. The date for this sample, A.D. 1210–1390, indicates that the penultimate earthquake on the Aeropuerto fault occurred prior to A.D. 1390.

To provide a closer estimate of the age of this event, we attempted to correlate the Quaternary stratigraphy between the trenches and a streambank exposure nearby and then develop a model that integrates the local geomorphology and Quaternary stratigraphy. A few hundred meters east of the Aeropuerto fault, about 150 m southeast of shoreline 2, is a 1.5-m-high stream bank exposure of Holocene lacustrine, volcanic, and fluvial deposits, which we logged in detail (Figs. 3 and 8). The lower part of the sedimentary sequence comprises typical lacustrine sediments (unit S-8), which are overlain by and interfinger with reworked volcanic material (unit S-7), indicating a transition to near-shore conditions and a substantial influx of volcanic sediments. These conditions give way to a marsh environment (unit S-6), consistent with a further fall in lake level to a height below that of this exposure, impeding drainage. Unit S-6 is overlain by overbank deposits (units S-5, S-3, S-2, and S-1) indicative of fluvial deposition. A further fall in lake level to the present elevation has been accompanied by local down-cutting, which has exposed this record of sedimentation.

We propose that these sediments record a change in depositional environment from the high stand of the lake that produced shoreline 1, to impeded drainage conditions and a marsh environment associated with the formation of shoreline 2. Finally, the shoreline 2 berm was breached, and the modern through-going drainage system and current lake level were established. If this model is correct, the radiocarbon age of sample 7 (Table 2) collected from unit S-6 (Fig. 7) provides a minimum estimate for the age of formation of shoreline 2 (and therefore a minimum age for occurrence of the penultimate rupture event) of 1830–1990 calibrated years B.P.

The shoreline 2 berm is composed of volcanic sand that was reworked by lacustrine shoreline processes. This indicates that the shoreline 2 berm formed after an influx of volcanic sediments in and near the lake. The youngest volcanic unit mapped in this area is known as the Masaya Tuff and is estimated to be 2.3 to 6.5 ka (Bice, 1980). The penultimate rupture of the Aeropuerto fault occurred before the formation of shoreline 2. If shoreline 2 formed shortly after the eruption of the Masaya Tuff, the penultimate earthquake occurred before about 2000 years B.P., consistent with our interpretation of the streambank exposure and the age of sample 7.

We suggest that the shorelines represent temporary high

stands of Lake Managua associated with the damming of the lake outlet in the aftermath of large eruptions, probably from Masaya Caldera. The reworked volcanic sediments exposed in trench 1 (units T1-7A, T1-7B, and T1-7C, Fig. 5) and trenches 2 and 3 (units T2/3-6, Figs. 6 and 7) are probably derived from the products of those eruptions. However, the reworked volcanoclastic units exposed in trench 1 were not deposited at the same time as those exposed in trenches 2 and 3. Those exposed in T2 and T3 were deposited later than those deposited in T1. We do not know how much time elapsed between the eruption or eruptions and the deposition of the reworked volcanics exposed in the trenches and stream-bank exposure. The penultimate rupture of the Aeropuerto fault occurred after the deposition of the reworked volcanic units in trench 1, and before the formation of shoreline 2. If both volcanoclastic units are derived from the Masaya Tuff, the penultimate earthquake occurred between approximately 2 and 6.5 ka. No lacustrine units are exposed in trench 1, indicating that the volcanoclastic units in trench 1 postdate the lacustrine high-stand of shoreline 1 and implying that lacustrine units are present beneath the floor of the excavation.

In trenches 2 and 3, we interpret lacustrine deposits (unit T2/3-8) similar to those observed in the streambank exposure, to be deposited when shoreline 1 was the lake edge. These lacustrine deposits underlie the volcanic unit (unit T2/3-6) that is reworked to form the base of the shoreline 2 berm. The fault exposed between meters 0 and 1 in trench 2 (Fig. 6), and between meters 3 and 4 in trench 3 (Fig. 7) terminates between units T2/3-8 and T2/3-6. This relationship indicates that the penultimate surface rupture may have occurred after the deposition of unit T2/3-8, but prior to the deposition of unit T2/3-6. Sample 8, collected from unit T2/3-8 in trench 3 (Fig. 7), provides a maximum age for this event of 6440 years B.P. (Table 2).

Lake Managua Shorelines and Estimates of Aeropuerto Fault Slip Rates

The two former shorelines of Lake Managua both formed across the Aeropuerto fault. If our stratigraphic model is correct, shoreline 1 was abandoned sometime in the last 6.4 ka, and prior to 1.9 ka. This is consistent with previous studies in which lake deposits were documented about 6 m above the modern shoreline east of the Cofradia fault near Tipitapa (Fig. 2). Those deposits were dated at about 4000 (shells) and 6000 radiocarbon years (peat) (Dames and Moore-Lamsa, 1978). Shoreline 1 is preserved continuously along the southern margin of Lake Managua west of the Aeropuerto fault, but is absent east of the Aeropuerto fault within the Airport graben (Fig. 3). This indicates that the shoreline is buried within the Airport graben on the eastern, down-dropped side of the fault.

Two detailed topographic profiles across the fault scarp south of shoreline 2 (p2 and p3 in Figs. 3 and 9) indicate a scarp height of 2 to 3 m. Trench 1 shows that fluvial deposition has occurred on both sides of the fault since shoreline

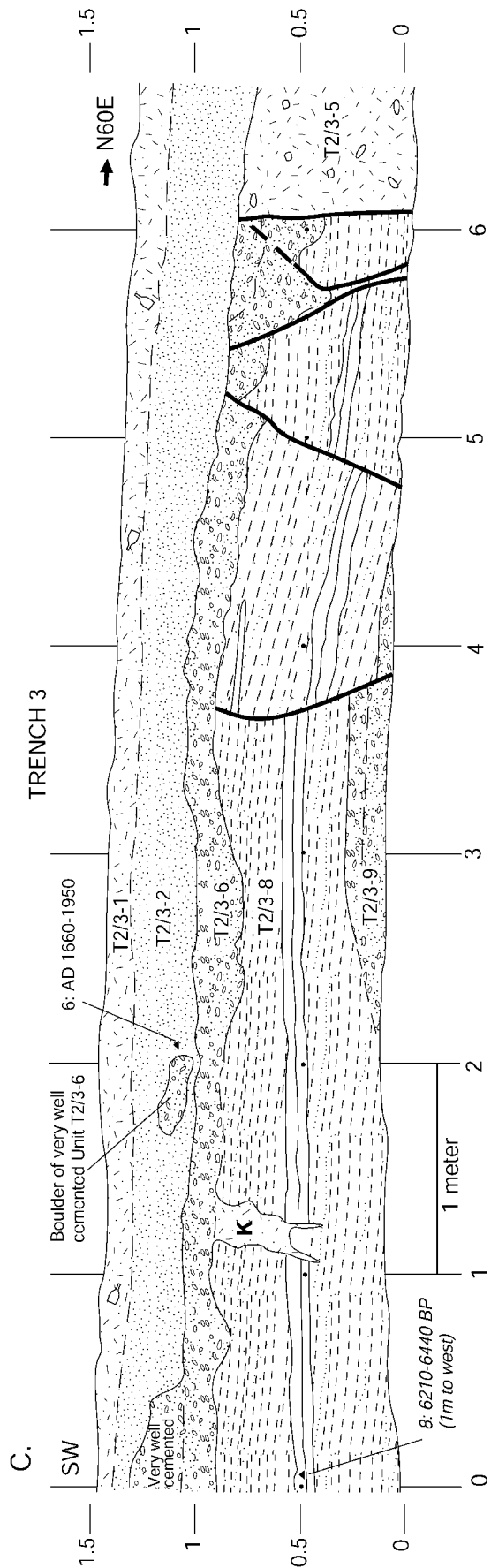


Figure 7. Log of trench 3. Commentary as under Fig. 6.

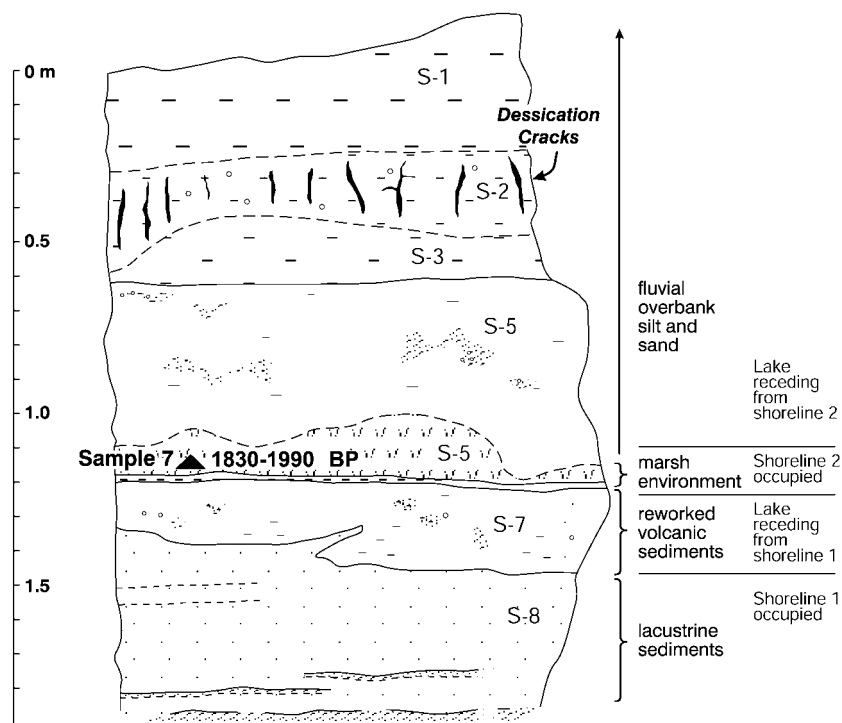


Figure 8. Log of streambank exposure (see Fig. 3) that records a transition from lacustrine conditions (unit S-8) associated with shoreline 1, through a fall in lake level and a volcanic eruption (unit S-7) that we interpret to be associated with the formation of shoreline 2. A marsh environment (unit S-6) subsequently formed behind the shoreline 2 berm. The fluvial overbank deposits (units S-5, S-3, S-2, and S-1) are associated with breaching of the berm and further retreat of the lake. We correlate unit S-8 with unit T2/3-8 in trenches 2 and 3, and unit S-7 with unit T1-7 in trench 1. The age of unit S-6 (1830–1990 calibrated years B.P.) provides an estimate for the time of formation of shoreline 2 (unit T2/3-6 exposed in trenches 2 and 3) and a minimum age for the volcanic eruption and the penultimate surface rupture on the Aeropuerto fault.

1 was abandoned post 6400 years ago (Fig. 5) and approximately 2 m vertical offset is recorded on unit T1-7A. Shoreline 1 is buried on the eastern side of the fault, so we infer that 2 to 3 m is the minimum amount of vertical slip since that time. This gives a minimum slip rate of 0.3 to 0.5 mm/yr.

Shoreline 2 intersects the Aeropuerto fault several hundred meters north of shoreline 1 (Fig. 3), but the two shorelines merge approximately 1 km farther west. The geometries and relative positions of the modern shoreline and shoreline 2 reflect probable footwall uplift and local tilting of the region west of the Aeropuerto fault. Shoreline 2 is present on both sides of the Aeropuerto fault (Fig. 3). Figure 9A is a profile constructed across the fault along the inner base of the berm. This profile shows a scarp height across the fault of between about 1.0 and 1.7 m, and tilting of the surface farther west.

If our model of the local Quaternary stratigraphy is correct, the shoreline 2 berm formed about 2 ka ago. The berm width is greatest adjacent to the downthrown side of the fault, implying that sediment accumulated at the base of a pre-existing scarp. This geometry implies that the measured scarp height (profile p1, Fig. 9A) represents a maximum estimate of vertical fault slip since the time the berm formed. A maximum of 1.0 to 1.7-m slip in 2000 years gives a maximum vertical slip rate estimate of 0.5 to 0.9 mm/yr. A similar rate is indicated by a 1.0-m offset across the scarp on the younger lakebed surface north of shoreline 2 (profile p4, Fig. 9). This surface is younger than the berm and therefore implies a minimum vertical slip rate estimate of 0.5 mm/yr in less than 2000 years.

The abrupt changes in the thicknesses of units across the fault splays shown in trench 1 (e.g., unit T1-7B across F5, Fig. 5), and the observed historical, left-lateral slip of nearby active faults, all suggest a component of horizontal slip on the Aeropuerto fault; however, the sense and amount of lateral slip across the Aeropuerto fault remains uncertain. We suggest that if the shoreline 2 berm had accumulated as much as 10 m of lateral offset we would be able to detect it, so the lateral slip rate must be less than about 5 mm/yr. The role of the Aeropuerto fault in the overall structure and kinematics of the Managua Graben may differ from that of the strike-slip faults to the west, and may instead be linked to the evolution of the Masaya Caldera located farther south (Fig. 2).

Conclusions

The Aeropuerto fault forms the western boundary of the Airport graben, the deepest part of the Managua Graben. The most recent earthquake on this fault occurred between A.D. 1650 and 1810. The historical record suggests this may have been the earthquake of 1663, 1764, or an event in 1772 associated with the largest historical eruption of Masaya Caldera. The penultimate event most likely occurred 2000 to 6440 years B.P.

We estimate the vertical slip rate on the Aeropuerto fault to be 0.3 to 0.9 mm/yr, based on vertical offsets of the two abandoned shorelines, and our estimate of their ages at less than 6.4 ka and approximately 2 ka, respectively. Although we collected some information that strongly implies a component of horizontal slip, we cannot be certain of the sense

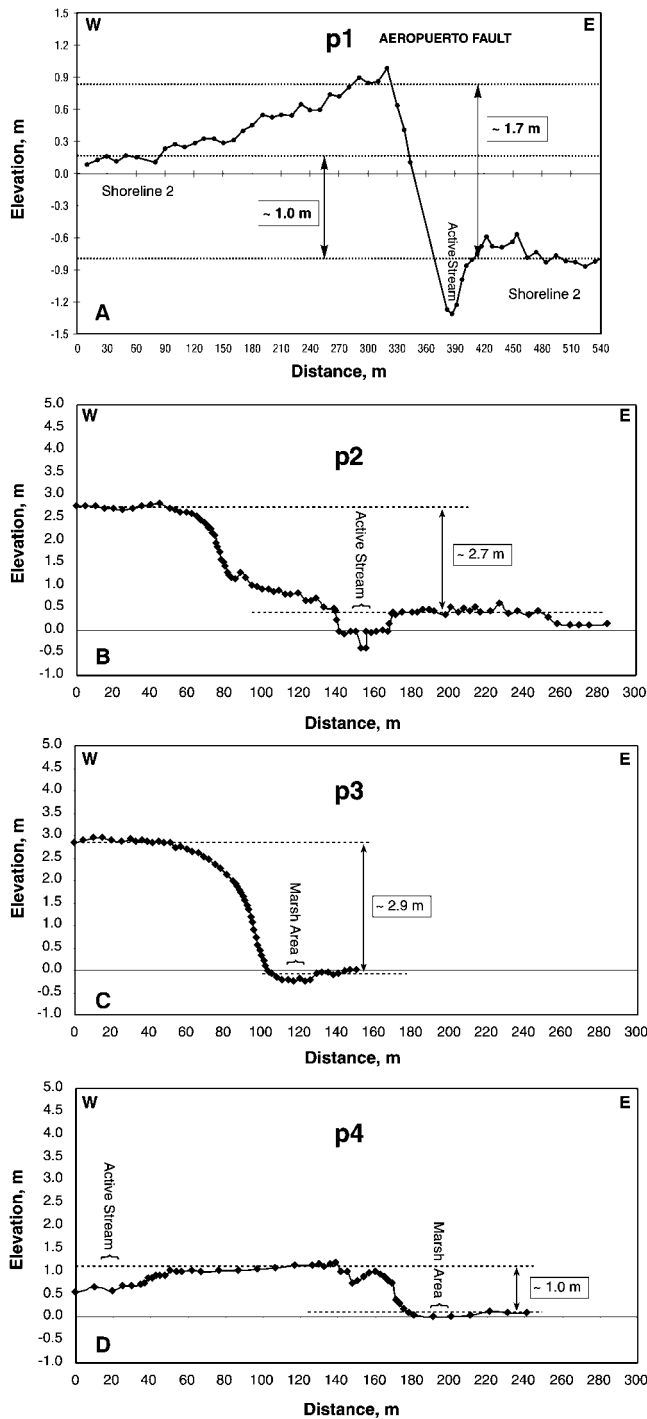


Figure 9. (A) Profile along the landward base of shoreline 2 (see p1 in Fig. 3) showing 1- to 1.7-m offset across the Aeropuerto fault. This represents the vertical offset across the fault since the berm formed. (B,C,D) Topographic profiles across the Aeropuerto fault. P2 and P3 are on the older lakebed delimited to the south and the north by shoreline 1 and 2, respectively. P4, on the younger lakebed south of the 1998 shoreline, records a vertical offset much smaller than p2 and p3, thus implying a shorter history of deformation.

and amount of lateral slip. Our analysis of the Aeropuerto fault and a comparison with similarly oriented active faults in Managua suggest that lateral slip must be accumulating at a rate of less than 5 mm/yr. The available data imply that fault rupture events occur at intervals of more than 1000 years to produce the observed displacements. Additional data on slip rate and timing of paleoearthquakes are needed to better assess the Holocene behavior of the Managua faults and to investigate the influence of magmatic processes on the nature of faulting in the Managua Graben.

Acknowledgments

Fieldwork was conducted during a Central American workshop in paleoseismology held in Managua, 16–22 March 1998. The workshop was facilitated by Centro de Coordinación para la Prevención de Desastres Naturales en América Central (CEPRENAC), the Norwegian Agency for Development Cooperation (NORAD), and host organization Instituto Nicaraguense de Estudios Territoriales (INETER). Workshop instructors were supported by the International Lithosphere Program (ILP), the U.S. Geological Survey, and Istituto Nazionale di Geofisica e Vulcanologia (INGV), Rome, Italy. We thank Xavier Amador and Philip Carthew for preparing the figures for this paper. Insightful reviews by Kelvin Berryman, Paul Mann, Jim McCalpin, and Buddy Schweig significantly improved the manuscript.

References

- Bevis, M., and B. L. Isacks (1984). Hypocentral trace surface analysis: probing the geometry of the Benioff zones, *J. Geophys. Res.* **89**, 6153–6170.
- Bice, D. C. (1980). Tephra stratigraphy and physical aspects of recent volcanism near Managua, *Ph.D. Thesis*, University of California at Berkeley, 422 pp.
- Brown, R. D., P. L. Ward, and G. Plafker (1973). Geologic and seismologic aspects of the Managua, Nicaragua, earthquakes of December 23, 1972, *U.S. Geol. Surv. Profess. Pap.* **838**, 34 pp.
- Carr, M. J. (1976). Underthrusting and Quaternary faulting in Central America, *Geol. Soc. Am. Bull.* **87**, 825–829.
- Coburn, A., and R. Spence (1992). *Earthquake Protection*. Wiley, New York.
- Cowan, H. A., M. N. Machette, X. Amador, K. S. Morgan, R. L. Dart, and K. Haller (2000). *Map and Database of Quaternary Faults In the Vicinity of Managua, Nicaragua, U.S. Geol. Surv. Open-File Rep. 00-0437* (released January 2002).
- Dames and Moore-Lamsa (1978). Informe final del Estudio Geológico de las Ciudades del Sistema Metropolitano, Vice Ministerio de Planificación Urbana, Gobierno de la Republica de Nicaragua.
- DeMets, C., R. G. Gordon, D. F. Argus, and S. Stein (1994). Effect of recent revisions to the geomagnetic reversal time scale on estimate of current plate motions, *Geophys. Res. Lett.* **21**, 2191–2194.
- Dewey, J. W., and S. T. Algermissen (1974). Seismicity of the Middle America arc-trench system near Managua, Nicaragua, *Bull. Seism. Soc. Am.* **64**, 1033–1048.
- Geographic Air Survey Limited (1996). Aerial photo series, Series 69603028: Line 12 (No. 93–97) and Line 11 (No. 46–49), scale 1:5,000, Managua (held at INETER, Managua).
- Hernandez, Z., K. Atakan, and J. Havskov (1994). Seismicity and tectonics near Managua, Nicaragua, Report 1–16, Reduction of Natural Disasters in Central America, Establishment of Local and Regional Data Centers, CEPREDENAC/Institute of Solid Earth Physics, Bergen, Norway.
- INETER (1987). Topographic map series, scale 1:10,000, Managua and Masaya (held at INETER, Managua).

- Instituto Geográfico Nacional (1972). Mapa Geológicos de la Región Occidental de Nicaragua: Instituto Geográfico Nacional (held at INETER, Managua) scale 1:250,000.
- Leeds, D. J. (1974). Catalog of Nicaraguan earthquakes, *Bull. Seism. Soc. Am.* **64**, 1135–1158.
- Malfait, B. T., and M. G. Dinkelman (1972). Circum-Caribbean tectonic and igneous activity and the evolution of the Caribbean plate, *Bull. Geol. Soc. Am.* **83**, 251–272.
- Mann, P., C. Schubert, and K. Burke (1990). Review of Caribbean neotectonics, in *The Caribbean Region*, G. Dengo and J. E. Case, (Editors), *The Geology of North America*, vol. H, Geological Society of America, Boulder, Colorado.
- Manton, W. I. (1987). Tectonic interpretation of the morphology of Honduras, *Tectonics* **6**, 633–651.
- McBirney, A. R., and H. Williams (1965). Volcanic history of Nicaragua, *Univ. Calif. Publ. Geol. Sci.* **55**, 1–65.
- Protti, M., F. Guendel, and K. McNally (1995). Correlation between the age of the subducting Cocos plate and the geometry of the Wadati–Benioff zone under Nicaragua and Costa Rica, in *Geological and Tectonic Development of the Caribbean Plate Boundary in Southern Central America*, P. Mann (Editor), *Geol. Soc. Am. Spec. Pap.* 295, 309–326.
- Stoiber, R. E., and M. J. Carr (1973). Quaternary volcanic and tectonic segmentation of Central America, *Bull. Volcanol.* **37**, 304–324.
- Stuiver, M., P. J. Reimer, E. Bard, J. W. Beck, G. S. Burr, K. A. Hughen, B. Kromer, G. McCormac, J. van der Plicht, and M. Spurk (1998). INTCAL98 radiocarbon age calibration, 24,000–0 cal BP, *Radiocarbon* **40**, 1041–1083.
- Sultan, D. I. (1931). The Managua earthquake, *Mil. Eng.* **23**, 354–361.
- Sussman, D. (1985). Apoyo Caldera, Nicaragua: a major Quaternary silicic eruptive center, *J. Volcanol. Geotherm. Res.* **24**, 249–282.
- van Wyk de Vries, B. (1993) Tectonics and magma evolution of Nicaraguan volcanic systems, *Ph.D. Thesis*, The Open University, London, 276 pp.
- Ward, P. L., J. Gibbs, D. Harlow, and A. Aburto (1974). Aftershocks of the Managua, Nicaragua, earthquake and the tectonic significance of the Tiscapa fault, *Bull. Seism. Soc. Am.* **64**, 1017–1029.
- Weinberg, R. F. (1992). Neotectonic development of western Nicaragua, *Tectonics* **11**, 1010–1017.
- White, R. A. (1991) Tectonic implications of upper-crustal seismicity in Central America, in *Neotectonics of North America*, D. B. Slemmons, E. R. Engdahl, M. D. Zoback, and D. Blackwell (Editors) Geological Society of America, Boulder, Colorado 323–338.
- White, R. A., and D. H. Harlow (1993). Destructive upper-crustal earthquakes of Central America since 1900, *Bull. Seism. Soc. Am.* **83**, 1115–1142.
- Williams, S. N. (1983). Geology and eruptive mechanisms of Masaya Caldera complex, Nicaragua, *Ph.D. Thesis*, Dartmouth College, Hanover, New Hampshire, 169 pp
- Woodward-Clyde Associates (1975). Investigation of active faulting in Managua, Nicaragua, and vicinity. Final report to Vice Ministerio de Planificación Urbana, Gobierno de la Republica de Nicaragua.
- Independent Consultant
Apartado 2561
Zona 9A, Panama City
Republic of Panama
(H.C.)
- U.S. Geological Survey
345 Middlefield Road, MS 977
Menlo Park, California 94025
(C.P.)
- Istituto Nazionale di Geofisica e Vulcanologia
Via di Vigna Murata, 605
00143 Rome
Italy
(D.P., P. di M.)
- Instituto Nicaraguense de Estudios Territoriales
Apartado 2110
Managua, Nicaragua
(W.S.)
- Participants of the Central American Workshop in Paleoseismology, Managua, 16–22 March 1998:* Gustavo Altamirano, Kuvvet Atakan, Nelson Buitrago, Hilmar Bungum, Manuel Caballo, Mauricio Darce, Omar Flores, Miguel Guevara, Glenn Hodgson, Ernesto Luna, Evelyn Martínez, William Martínez, Eduardo Mayorga, Jimmy Mercado, Alonso Miranda, Franklin Moore, Jose Rivas, Dionísio Rodríguez, Noel Rodríguez, Guillermo Salazar, Fabio Segura, Gerardo Silva, Roberto Solis, Waldo Taylor, and Carlos Tenorio